

## Color Enhancement of Rambutan Peel Anthocyanins Extracts using Co-Pigmentation with Gallic Acid for pH-Sensitives Dye

Arum Widyastuti Perdani<sup>1,2</sup>, Arima Diah Setiowati<sup>1</sup>,  
Bambang Purwono<sup>3</sup> and Supriyadi Supriyadi<sup>1,\*</sup>

<sup>1</sup>Department of Food and Agricultural Product Technology, Faculty of Agricultural Technology, Universitas Gadjah Mada, Yogyakarta 55281, Indonesia

<sup>2</sup>Applied Culinary Arts Study Program, Faculty of Vocational Studies, Universitas Negeri Yogyakarta 55893, Indonesia

<sup>3</sup>Department of Chemistry, Faculty of Mathematics and Natural Sciences, Universitas Gadjah Mada, Yogyakarta 55281, Indonesia

(\*Corresponding author's e-mail: suprif248@ugm.ac.id)

Received: 13 December 2024, Revised: 2 January 2025, Accepted: 9 January 2025, Published: 20 February 2025

### Abstract

Rambutan peels typically contain anthocyanins that can be utilized as pH-sensitive dye for intelligent food packaging. Therefore, this study aimed to isolate anthocyanins from rambutan peels and investigate their co-pigmentation with gallic acid (GA) to enhance color intensity while maintaining a pH sensitivity. Rambutan peel anthocyanins extracts (RPAE) were extracted using ultrasound-assisted extraction with 0.2 % citric acid in 96 % ethanol. The purification of RPAE was carried out using a chromatography column with Sephadex LH-20 as the stationary phase. Co-pigmentation was then performed using GA at various molar ratios of RPAE to GA (1:0, 1:100, 1:200, 1:300, 1:400 and 1:500). The results showed that the purification process with Sephadex LH-20 increased the anthocyanins content of RPAE to 157.50 mg CyE/100 g extract. After purification, RPAE was found to primarily consist of cyanidin 5-O-glucoside, delphinidin-3-O-glucoside, cyanidin 3-O-galactoside, delphinidin (aglycon), cyanidin-3-O-glucoside, pelargonidin 3-O-glucoside, and cyanidin (aglycon). Co-pigmentation with GA significantly reduced the degradation of total anthocyanin content compared to native RPAE during the 7-day observation period. Additionally, co-pigmentation with GA enhanced color intensity, as demonstrated by a decrease in the L\* value across pH 1-10, an increase in the a\* and b\* values at low pH, and a decrease in the a\* and b\* values at high pH. However, compared to non-co-pigmentation, co-pigmentation with GA exhibited more pronounced color differences across varying pH levels, marked by higher a\* at low pH and lower b\* and L\* at high pH. The interaction between GA and RPAE, presumably via hydrogen bonding comprising the carbonyl group of RPAE and GA, produced hyperchromic and bathochromic effects. These findings indicate that co-pigmentation with GA enhances the pH sensitivity of RPAE, making it a promising candidate for developing intelligent food packaging systems that can visually indicate changes in pH, such as monitoring food spoilage or freshness.

**Keywords:** Anthocyanins, Rambutan peels, Intelligent packaging, Purification, Sephadex LH-20, Co-pigmentation, Gallic acid

### Introduction

Food packaging is often used to preserve and extend shelf life, as well as monitor food freshness through intelligent packaging systems such as colorimetric sensors [1]. These systems alter color in

response to interactions with food or its surroundings, providing a visual signal of freshness throughout distribution and storage [2]. In colorimetric intelligent packaging, a chemosensor component is responsible for indicating food freshness through color changes. A

chemosensor consists of 2 key components, namely a sensitive dye and a carrier matrix [3]. The sensitive dye changes color in response to interactions with total volatile basic nitrogen (TVB-N) [4], pH [5], CO<sub>2</sub> [6], and ethylene [7], which are indicators of product degradation. Meanwhile, the carrier matrix, commonly a biopolymer, immobilizes the dye [3].

Sensitive dye for intelligent packaging can either be synthetic or natural. Several studies have shown that synthetic dye is progressively being avoided due to its toxic effects and possible adverse impacts on health and the environment [5,8]. Therefore, this material is increasingly replaced by natural dye derived from plants, which are pH-sensitive and comply with food safety and environmental sustainability standards [5]. Natural dye that can be utilized as chemosensor for intelligent packaging include anthocyanins, betanin, betalains, carotenoids, chlorophyll, and curcumin [9-12]. Among these, anthocyanins are particularly known for their wide pH-responsive color range [11,12], leading to high suitability for chemosensors in intelligent packaging.

Anthocyanins are water-soluble pigments classified within the phenolic and flavonoid categories, found in roots, stems, leaves, peels, and flowers [13]. These pigments alter their color in response to pH changes due to structural modifications [11,13]. At pH 1-3, anthocyanins exist as flavylium cations. After losing H<sup>+</sup>, these compounds form a purple quinoidal base, which can further deprotonate to an anionic quinoidal base, appearing blue or green, depending on H<sup>+</sup> loss. The carbinol pseudobase is colorless and forms chalcone, a yellow-colored structure with an open ring, upon further deprotonation [13]. These chromatic changes can serve as a colorimetric signal in intelligent packaging. Anthocyanin-rich materials, especially those with red, purple, and blue hues, are abundant in nature. However, anthocyanin-rich byproducts, such as red rambutan peels, remain underutilized. In Indonesia, over 400,000 tons of rambutan peels are generated as waste annually [14], offering great potential as a novel resource. Anthocyanins contents of rambutan peels are comparable to those of other well-known sources like purple sweet potato and purple corn [15]. Rambutan peels contain 181.3 - 983 mg/100 g of anthocyanins, depending on the variety [16,17], while purple sweet potato and purple corn have 46.5 - 56.7 mg/100 g [18]

and 55.2 mg/100 g [15], respectively. Studies have identified anthocyanin derivatives, such as delphinidin in Brazilian rambutan peels [17] and pelargonidin in Mexican varieties [19].

Despite their potential, anthocyanins derived from natural sources, including rambutan peels, face limitations such as low color intensity and poor stability against temperature, light, and time [6,12,20]. To address these limitations, co-pigmentation has emerged as an effective strategy to enhance both the stability and color intensity of anthocyanins [21-22]. This process involves  $\pi$ - $\pi$  interactions between electron-rich co-pigments and the flavylium cation [23-24]. Co-pigmentation can be categorized based on the materials used, such as metal-based and non-metal-based co-pigments, and by the type of interaction, such as intermolecular interactions or intramolecular bonds with chromophore groups [25]. Non-metal co-pigmentation, particularly with phenolic acids, has been reported to stabilize a wider range of anthocyanin types and is regarded as non-toxic and safer for human use compared to metal-based co-pigments [21,26].

Phenolic acids, phenols that have lost a proton from their hydroxyl group and are rich in  $\pi$ - $\pi$  electrons, interact with anthocyanin flavonoid ions, protecting them from nucleophilic attack and enhancing their color stability through antioxidant activity [26,27]. Among various phenolic acids, GA contains the highest number of hydroxyl groups [27]. Several studies have shown that it is rich in  $\pi$ - $\pi$  electrons, enabling the compound to form stronger interactions with anthocyanins ions than other phenolic acids [27]. In addition to the type of co-pigment, the molar ratio of anthocyanins to co-pigments is also critical. Co-pigmentation arises from anthocyanins and co-pigments via molecular interactions [28]. The optimal molar ratio depends on the specific anthocyanins composition in the sample. Therefore, selecting the appropriate co-pigment and molar ratio will enhance color intensity and maintain sensitivity to TVB-N and pH changes.

It has been reported that RPAE is a potential pH-sensitive dye, and GA acts as a co-pigment. However, the characterization of RPAE and its co-pigmentation with GA remains limited, particularly with regard to its stability and application as a sensitive dye for intelligent packaging. To address these gaps, the present study aims to characterize RPAE and evaluate its co-pigmentation

with GA to enhance color intensity and pH sensitivity. This research aligns with the principles of Green Technology and the Sustainable Development Goals by focusing on reducing food and agricultural waste while improving food safety through freshness monitoring. These developments have significant potential for use as food freshness indicators, contributing to sustainable and innovative food packaging solutions.

## Materials and methods

### Chemicals and reagents

RPAE was obtained from the Binjai rambutan variety with red-colored peels harvested between November 2023 and January 2024 in Bantul, Yogyakarta, Indonesia. The materials used for anthocyanins extraction were citric acid (Sigma-Aldrich G7384, Germany) and ethanol (Sigma-Aldrich, Germany). Furthermore, Sephadex LH-20 (CAS No. 9041-37-6, Nanjing Duly Biotech) was used for purification, while gallic acid (GA) (Sigma-Aldrich, Germany) was used for co-pigmentation. Analytical-grade reagents were applied for all analyses in this study.

### Ultrasound-assisted extraction of RPAE

Fresh rambutan peels were blanched using water blanching at 50 °C for 2.5 min to inactivate enzymes that degraded the color [29,30]. Subsequently, the peels were dried at 50 °C for 24 h using cabinet drying, ground into powder, and sieved through a 40-mesh screen (Haver & Boecker, 59302 OELDE, Germany). The characteristics of the rambutan peel powder were as follows, the moisture content of  $5.89 \pm 0.41$  % using AOAC, 1995 [31],  $L^*$  value of  $55.98 \pm 1.74$ ,  $a^*$  value of  $11.18 \pm 0.67$ ,  $b^*$  value of  $0.67 \pm 1.55$  using chromameter (CR-400 Konica Minolta, Japan), and total anthocyanins content of  $23.27 \pm 1.39$  mg CyE /100g (DB) using Giusti and Wrolstad (2001) methods [32]. This powder was then extracted using 96 % ethanol and 0.2 % citric acid in a 1:20 ratio through Ultrasound-Assisted Extraction (UP200St, Hielscher Ultrasonics GmbH, Teltow, Germany) [17]. The extraction was performed using a 7 mm diameter probe at 200W and 20 kHz, maintaining a temperature of 50 °C for 20 min. Furthermore, the temperature was controlled with a Frigiterm-TFT-10 thermostat water bath (J.P. Selecta S.A., Barcelona,

Spain). After extraction, the extract was immediately centrifuged at  $2,600 \times g$  for 15 min to obtain a supernatant containing the anthocyanins extract and was subsequently filtered with Whatman No. 1 filter paper. This extract was concentrated using rotary evaporation and stored at  $-18$  °C for further analysis and purification.

### Purification of RPAE

Anthocyanins were purified using Sephadex LH-20 [33]. RPAEs were loaded into a column  $20 \times 300$  mm<sup>2</sup> of Sephadex LH-20 that had been activated by passing deionized water. In this study, Sephadex LH-20 served as the stationary phase, while 90 % methanol with 0.01 % HCl was used as the mobile phase. The fractions from the purification process had their solvents evaporated using a rotary evaporator at 40 °C [34] to remove ethanol, and the remaining water solvent was removed using a freeze-dryer. Finally, the anthocyanin extract was stored at  $-18$  °C for further analysis and co-pigmentation.

### Co-pigmentation RPAE using GA

Co-pigmentation between RPAE and GA was conducted using molar ratios of 1:0, 1:100, 1:200, 1:300, 1:400 and 1:500 (RPAE: GA). The solutions of RPAE and GA were prepared using deionized water. Anthocyanin solutions were prepared at a concentration of 0.02 mM in deionized water containing 0.01 % HCl, amounting to 10 mL. At the calculated molarity, GA was added in amounts corresponding to 0, 100, 200, 300, 400 and 500 times the molar number of anthocyanins. Subsequently, the mixture was stirred using a magnetic stirrer at 750 rpm for 20 min. The total volume of the solution was adjusted to 15 mL. After homogenization, the solution was set aside to stand for 1 h to allow co-pigmentation to occur. Following this process, co-pigmented RPAEs with GA were obtained [35].

### Total anthocyanins content (TAC)

Total anthocyanins contents (TACs) were determined using the pH differential method [32] and tested on rambutan powder for initial material characterization, ultrasonic RPAE, purified RPAE, and RPAE-GA co-pigmentations. The samples were dissolved in methanol, diluted 1:1 with KCl buffer (pH

1) and sodium acetate buffer (pH 4.5) and allowed to equilibrate for 15 min. Furthermore, absorbance at 510 and 700 nm was measured using a spectrophotometer (Genesys 10S UV-Vis, Thermo Scientific, USA). Total anthocyanins concentration (mg CyE/100 g) was calculated using Eq. (1).

$$A = (A_{\max} - A_{700})_{\text{pH1}} - (A_{\max} - A_{700})_{\text{pH4,5}}$$

$$\text{Total Anthocyanins (mg/100 g)} = \frac{(A \times \text{MW} \times \text{DF} \times 1000 \times 100)}{(\epsilon \times L \times m)} \quad (1)$$

A signified the absorbance difference (510 - 700 nm) between pH 1 and 4.5, MW depicted the molecular weight of cyanidin-3-glucoside (449.2 g/mol), DF was the dilution factor,  $\epsilon$  was the molar absorptivity (26,900 mol/L·cm), L depicted the cuvette path length (1 cm), and m was the sample weight (g) [32].

#### Total phenolic content (TPC)

Total phenolic contents (TPCs) were measured using the Folin-Ciocalteu reagent according to the method used by Klongdee and Klinkesorn (2022) [36]. RPAEs were diluted with distilled water, mixed with Folin-Ciocalteu reagent (0.2 mL), and distilled water (2.6 mL), and reacted for 6 min. Subsequently, 7 % sodium carbonate (2 mL) was added, and the mixture was stored in the dark for 90 min. The color was measured at 750 nm using a spectrophotometer (Genesys 10S UV-Vis, Thermo Scientific, USA). GA solution was used for the standard curve, and results were expressed as milligrams of GA equivalents per gram [36].

#### Liquid chromatography-high resolution mass spectra (LC-HRMS)

RPAE was identified using LC-HRMS, which was obtained from Germany (Thermo Scientific™ Dionex™ Ultimate 3000 RSLC nano UHPLC coupled with Thermo Scientific™ Q Exactive™ High-Resolution Mass Spectrometer). Anthocyanins were dissolved in 96 % methanol containing 0.2 % citric acid to prepare a stock solution at a concentration of 20 mg/mL. Mobile phase A consisted of 0.1 % formic acid in water (v/v), while mobile phase B was 0.1 % formic acid in methanol (v/v). The analytical column used in this study was a Phenyl-Hexyl column (100×2.1 mm) (Germany) with a flow rate of 0.20 mL/min and an injection volume of 5  $\mu$ L. Furthermore, the flow gradient for the mobile

phases was set at, 0 to 2 min, 0.2 mL/min, 5 % B; 15 min, 0.2 mL/min, 60 % B; 22 to 25 min, 0.2 mL/min, 95 % B; and 25.1 to 30 min, 0.2 mL/min, 5 % B. The total working time in this study was 30 min. Full MS was performed at 70,000 FWHM resolution, and data-dependent MS2 was conducted at 17,500 FWHM. Ionization was performed using Heated Electrospray Ionization (H-ESI) in both positive and negative modes, and compound identification was conducted using Thermo Scientific™ Compound Discoverer Software 3.2. Furthermore, anthocyanins types were searched against a literature-based database [16,37]. Data processing and library database loading were performed using Proteome Discoverer 2.5 software. Target analysis was conducted by searching components in the library database based on mass, isotopic, and fragmentation patterns [38].

#### Color analysis

Chromatic color analysis was conducted using a chromameter (CR-400, Konica Minolta, Japan) equipped with a 0.8 cm aperture, and calibrated with a white plate ( $Y = 86.5$ ,  $x = 0.3168$ ,  $y = 0.3245$ ) [39]. Intelligent packaging color parameters were  $L^*$  (lightness),  $a^*$  (red-green), and  $b^*$  (yellow-blue), and total color difference ( $\Delta E$ ) was calculated using Eq. (2).

$$\Delta E^* = \sqrt{(a_n^* - a_0^*)^2 + (b_n^* - b_0^*)^2 + (L_n^* - L_0^*)^2} \quad (2)$$

where  $a_0^*$ ,  $b_0^*$ , and  $L_0^*$  corresponded to the initial color parameters of the anthocyanins extract without co-pigmentation and  $a_n^*$ ,  $b_n^*$ , and  $L_n^*$  represented the color parameters of the anthocyanins extract after co-pigmentation [40].

#### Determination of co-pigmentation and absorbance retention

The effect of co-pigmentation was assessed by measuring the absorbance of co-pigmented anthocyanins samples (400 - 700 nm) using a spectrophotometer (Genesys 10S UV-Vis, Thermo Scientific, USA). Furthermore, the bathochromic shift ( $\Delta\lambda_{\max}$ ) was determined as the shift in the maximum wavelength ( $\lambda_{\max}$ ) compared to the control with non-co-pigmented anthocyanins. The hyperchromic shift, suggesting the increase in absorbance, was calculated as

the co-pigmentation effect [24]. Spectrophotometric data was used to determine the co-pigmentation effect and bathochromic shift [28,41]. The co-pigmentation effect, also referred to as the hyperchromic effect, was determined using Eq. (3).  $M$  represented the co-pigmentation effect (hyperchromic effect) in %, where  $A$  was the absorbance at 520 nm of the sample with co-pigments, and  $A_0$  was the absorbance at 520 nm of the sample without co-pigments [41].

$$\Delta A (\%) = \frac{A-A_0}{A_0} \times 100 \quad (3)$$

The bathochromic shift was determined using Eq. (4), with  $\Delta\lambda_{\max}$  representing the difference between maximum absorptions of the sample with ( $\lambda_{\max}$ ) and without ( $\lambda_{\max 0}$ ) co-pigments [28].

$$\lambda_{\max} = \lambda_{\max} - \lambda_{\max 0} \quad (4)$$

The color intensity was determined using Eq. (5), with  $A_{420}$ ,  $A_{520}$ , and  $A_{620}$ , which represented the absorbance values at 420, 520 and 620 nm, respectively [41]

$$\text{Color intensity} = A_{420} + A_{520} + A_{620} \quad (5)$$

#### Fourier transform infrared (FTIR)

RPAEs, both with and without co-pigmentation using GA, were examined using Fourier Transform Infrared (FTIR) spectroscopy using the KBr pellet technique. FTIR spectra were recorded using a spectrometer within the wavenumber range of 400 to 4,000  $\text{cm}^{-1}$ . The obtained spectra facilitated the identification of potential interactions among the components within the film matrix. Furthermore, the spectrum was derived from the combination of 10 scans to enhance resolution and accuracy [39].

#### Statistical analysis

Statistical analysis used a paired T-test to evaluate crude and purified TAC and TPC. In the co-

pigmentation of RPAE with GA, molar ratios were selected as the independent variable. Subsequently, degradation, chromatic color, hyperchromic shift, hypochromic shift, color intensity, and FTIR were evaluated. The data were then analyzed using analysis of variance (ANOVA), preceded by tests for normality and homogeneity, followed by Duncan's Multiple Range Test (DMRT) at a 5 % significance level, using SPSS software (IBM SPSS Statistics, IBM Corp., Version 20.0). All sample measurements were conducted in triplicate. Data are presented as mean  $\pm$  standard deviation.

## Results and discussion

### TAC and TPC of RPAE

The TAC of RPAE after purification using Sephadex LH-20, as shown in **Table 1**, increased up to 157.50 mg/100 g CyE extract (db), representing a 22.28 % improvement. The purification process, using Sephadex LH-20, separated the extract based on molecular weight. Higher molecular weight compounds were eluted first, while lower molecular-weight compounds were retained in the column [33]. The previous study reported that anthocyanins extract purification using AB-8 resin and Sep-Pak C18 combined with Sephadex LH-20 could increase the purity from 4.58 to 90.96 % [42]. Higher purification in the previous study was because of the multiple purification stages. The single-stage purification of RPAE revealed almost similar TAC between Sephadex LH-20 and Amberlite XAD-7 resin columns. Rambutan peels from Ningning, China, were extracted using ethanol/water/acetic acid (60:39:1, v/v/v) solvent and purified using Amberlite XAD-7 resin column reaching 181.3 mg/100 g CyE [16]. Rambutan peels from Thailand were extracted using microwave-assisted extraction, gaining TAC up to  $318.28 \pm 5.56$  mg/g CyE [36]. Heat-assisted extraction yielded 5.75 - 13.95 mg/g and UAE 2.69 to 9.83 mg/g [17]. These differences were attributed to the different varieties and extraction techniques of rambutan used.

**Table 1** Characteristics of RPAE.

Sample	TAC (mg/ 100 g CyE)	TPC (mg GAE/100 g)
Crude	128.81 ± 2.16	39941.71 ± 869.02
Purification using Sephadex LH-20	157.50 ± 2.69*	38456.95 ± 276.74*

Value with an asterisk (\*) symbol indicates a significant difference between crude anthocyanins extract using a paired T-test. Different superscripts in the same column indicate significant differences ( $p < 0.05$ ) by Duncan's Multiple Range Test.

The TPC decreased from 39,941.71 to 38,456.95 mg GAE/100 g after purification using Sephadex LH-20 (**Table 1**). TPC decreased due to the purification process selectively separated anthocyanins from other ingredients that had molecular weights significantly different from theirs, including phenolics. The previous study reported that the TPC of Thailand rambutan peel extract up to  $333.01 \pm 5.84$  mg GAE/g extract or equivalent with 33,301 mg GAE/100 g extract [36]. This extraction using an ohmic heating technique with water for a holding time of 15 min yielded a value of  $329.46 \pm 26.98$  mg-GAE/g, which was equivalent to 32,946 mg GAE/100 g extract. Meanwhile, the use of 70 % ethanol resulted in a value of  $587.98 \pm 83.31$  mg-GAE/g, corresponding to 58,798 mg GAE/100 g extract [43]. The results revealed that the extract's phenolic content was higher compared to that of Thailand rambutan peel extract obtained using the ohmic heating technique with water but lower than the phenolic content achieved using the 70 % ethanol ohmic heating technique. These differences were attributed to the variations in rambutan

varieties and the extraction techniques used. The main compounds in Thai rambutan peels are geraniin, corilagin, ellagic acid, ellagic acid pentoside, and shikimic acid [36]. Additionally, the phenolic profile of rambutan peels from Brazil includes ellagitannin derivatives, geraniin isomers, ellagic acid, and delphinidin-O derivatives [17].

#### RPAE identification

**Table 2** shows anthocyanins found in rambutan peel, checked using LC-HRMS. The type anthocyanins found in RPAE were cyanidin 5-O-glucoside, delphinidin 3-O-glucoside, cyanidin 3-O-galactoside, delphinidin (aglycon), cyanidin-3-O-glucoside, pelargonidin 3-O-glucoside, and cyanidin (aglycon). The main ones in RPAEs were cyanidin-3-O-glucoside and delphinidin-3-O-glucoside. These are from cyanidin, delphinidin and pelargonidin groups. Cyanidin makes red to orange, delphinidin gives purple or blue, and pelargonidin gives orange colors [1].

**Table 2** Targeted identification of RPAE using LC-HRMS.

Formula	Common name	Parent compound	Molecular weight	Retention time (min)	Area
C <sub>21</sub> H <sub>21</sub> O <sub>11</sub>	<i>Cyanidin 5-O-glucoside</i>	2-(3,4-Dihydroxyphenyl)-3,7-dihydroxy-5-chromeniumyl β-D-glucopyranoside	449.10696	1.175	$2.45 \times 10^{+6}$
C <sub>21</sub> H <sub>21</sub> O <sub>12</sub>	<i>Delphinidin 3-O-glucoside</i>	Myrtillin	465.10312	8.295	$2.97 \times 10^{+7}$
C <sub>21</sub> H <sub>21</sub> O <sub>11</sub>	<i>Cyanidin 3-O-galactoside</i>	Ideain	449.10714	8.854	$2.40 \times 10^{+7}$
C <sub>15</sub> H <sub>11</sub> O <sub>7</sub>	<i>Delphinidin (aglycon)</i>	Delphinidin	303.04964	9.134	$1.43 \times 10^{+7}$
C <sub>21</sub> H <sub>21</sub> O <sub>11</sub>	<i>Cyanidin-3-O-glucoside</i>	Cyanidin-3-glucoside	449.10715	9.135	$3.09 \times 10^{+7}$
C <sub>21</sub> H <sub>21</sub> O <sub>10</sub>	<i>Pelargonidin 3-O-glucoside</i>	Callistephin	433.11262	9.748	$9.45 \times 10^{+6}$
C <sub>15</sub> H <sub>11</sub> O <sub>6</sub>	<i>Cyanidin (aglycon)</i>	Cyanidin	287.0549	9.748	$4.38 \times 10^{+6}$

Anthocyanins were glycosylated anthocyanidins, referring to anthocyanidins esterified with 1 or more sugar groups [1]. The 6 main anthocyanidins, including pelargonidin, cyanidin, delphinidin, peonidin, petunidin, and malvidin, differed in side chains. Sugar groups like glucose, galactose, and rhamnose could form mono or disaccharides, which were acylated, resulting in variations in hydroxyl and methoxyl groups, sugar positioning, and acylation degree [1]. Previous studies reported that anthocyanins in Brazilian rambutan peel were identified as delphinidin derivatives [17], while anthocyanins in Mexican rambutan peel were identified as pelargonidin derivatives [44].

#### Degradation of RPAE with GA as co-pigment

Figure 1 indicated the decrease in TAC up to 7 days at room temperature. RPAE pigmented with GA exhibited a slower reduction in anthocyanins content than those without co-pigmentation. The lowest reduction occurred on molar ratios of 1:300, 1:400 and 1:500, with no significant difference. Increasing GA concentration resulted in slower degradation due to intermolecular interactions between RPAE and GA,

which protected the anthocyanin chromophore from degradation. Co-pigmentation complexes prevented water molecules from nucleophilically attacking and forming chalcone structures [28]. GA was classified as a phenolic acid and abundant in hydroxyl groups, commonly found in various plants and foods [45]. Among the different phenolic acids, GA contained the most hydroxyl groups and was rich in  $\pi$ - $\pi$  electrons, enabling stronger interactions with anthocyanins ions than other phenolic acids [27]. This enhanced co-pigmentation formation with anthocyanins more effectively than other phenolic acids. GA had been identified as an anthocyanins co-pigment and was the most efficient agent in inhibiting anthocyanins degradation relative to other organic acids, including ferulic acid, tannic acid, and caffeic acid [26]. This provided the most preferable protection for purple sweet potato anthocyanins, although thermal protection remained limited [46]. Furthermore, it was also reported that black mulberry anthocyanins co-pigmented with GA improved thermal stability, with an anthocyanins-to-GA molar ratio of 1:75 and an activation energy value of 65.20 kJ/mol [35].

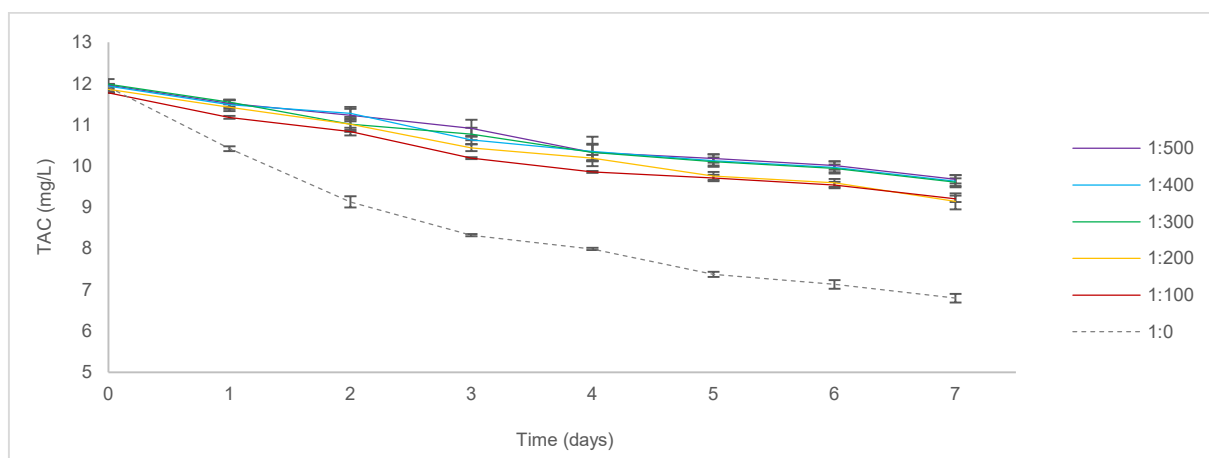


Figure 1 TAC degradation at room temperature in various molar ratios of GA as co-pigment.

#### Chromatic color properties of RPAE with GA as co-pigment

The color changes in the RPAEs were displayed in Figure 2(A). Furthermore, the color transitioned across pH levels from 1 to 10, shifting from pink to colorless, greenish-yellow, and eventually yellow. The anthocyanins found in rambutan peel extract were derivatives of cyanidin, delphinidin, and pelargonidin. Color alterations in this study were ascribed to structural

modifications in anthocyanins. At acidic pH, anthocyanins existed as flavylium cations, resulting in a red color, and converted into a purple quinoidal base by deprotonation, which further deprotonated into a blue-green anionic base. Reaction with water formed a colorless carbinol pseudobase, which, upon further deprotonation, opened the anthocyanins ring, producing a yellow chalcone [1,47,48]. RPAE using co-pigmentation with GA showed a deeper red color under

acidic conditions. At alkaline pH, the non-co-pigmented extract turned yellow, indicating chalcone formation, while the co-pigmented extract displayed a greener color, suggesting anionic quinoidal base formation [47-48]. As the molarity of GA increased, the solution became greener at pH 8 to 10. A previous study revealed that GA enhanced the color of anthocyanins in purple sweet potatoes by 19.1 % [46]. GA acted as a co-pigment for anthocyanins in *Berberis crataegina* [26].

The chromatic color parameters, comprising  $L^*$  (lightness, from bright to dark),  $a^*$  (green to red), and  $b^*$  (blue to yellow), were frequently applied to assess the susceptibility of anthocyanins extracts to pH-induced color shifts [28]. The  $L^*$  values tended to decrease as the molar ratio of anthocyanins to GA increased under both acidic (pH 1 to 4) and alkaline (pH 8 to 10) conditions (**Figure 2(B)**). A reduced  $L^*$  value in samples containing co-pigments signified a darker red color, presumably attributed to the co-pigments' protective

impact against anthocyanins degradation, thereby preventing color fading [28]. Furthermore, the  $L^*$  values showed an increase from pH 1 to 3 to pH 4 to 6, followed by a decrease under alkaline conditions.

**Figure 2(C)** indicated that within the pH range of 1 to 7, RPAE co-pigmented with GA demonstrated considerably higher  $a^*$  values ( $p < 0.05$ ) than those without co-pigmentation, particularly at molar ratios beginning at 1:300. This showed that co-pigmentation enhanced the intensity of the red color, correlating with increasing molar ratios. At pH 8 to 10, the  $a^*$  values of RPAE with GA decreased, indicating a shift towards a greenish color. Meanwhile, as shown in **Figure 2(D)**, the  $b^*$  values increased with higher molar ratios at pH 1, 2 and 8, while a decrease was observed at pH 7, 9 and 10. The decrease in  $b^*$  values suggested that the RPAE exhibited a hint of blue coloration. In **Figure 2(E)**, there was an increase in  $\Delta E^*$  values with the rising molar ratio of anthocyanins to GA as co-pigment.

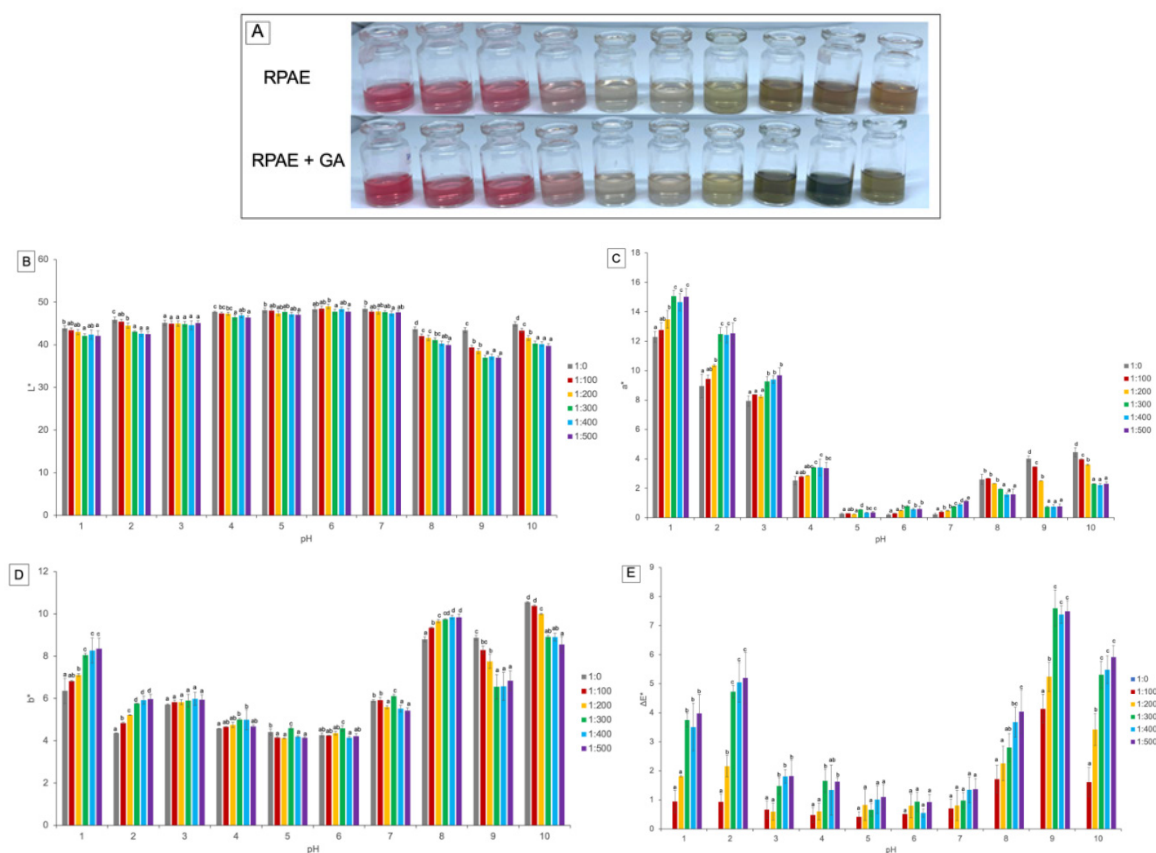


**Figure 2** Color of RPAE with GA as co-pigment under different pH levels.

The  $\Delta E^*$  values were calculated using the control sample of RPAE without co-pigmentation as a reference. These results indicated that higher  $\Delta E^*$

values corresponded to more noticeable color differences between the co-pigmented and non-co-pigmented samples, making the distinction more easily

perceivable to the naked eye. A study investigating the co-pigmentation of anthocyanins in blackberry wine with quercetin, syringic acid, and caffeic acid demonstrated a similar trend, characterized by a reduction in  $L^*$  values and an enhancement in both  $a^*$  and  $b^*$  parameters [28]. Similar results were also observed in the co-pigmentation of anthocyanins with chondroitin sulphate as an indicator film. Co-pigmentation with chondroitin sulphate resulted in a decrease in  $L^*$  values and an increase in  $a^*$  values [5].

Based on the analysis of  $L^*$ ,  $a^*$ ,  $b^*$  and  $\Delta E^*$ , RPAE with GA as a co-pigment exhibited more distinct and vibrant colors across various pH levels than RPAE without co-pigmentation. This enhancement is attributed to the formation of intermolecular interactions, which increased color intensity, as supported by the quantitative color intensity values and hyperchromic effects [41].

#### Hyperchromic effect, bathochromic shift, and color intensity of RPAE with GA as co-pigment

This study investigated the co-pigmentation of RPAE with GA. As shown in **Table 3** and **Figure 3**, GA induced a hyperchromic effect, as evidenced by increased absorbance values with higher molar ratios of co-pigment, demonstrating the formation of intermolecular interactions between anthocyanins and GA. A significant effect was observed starting from a

molar ratio of 1:300 (22.46 %), while no notable differences were detected between the ratios of 1:400 (22.61 %) and 1:500 (22.90 %). This suggested that the selected co-pigment, GA, absorbed negligible light in the visible spectrum, with the enhancement in the absorption of the model systems principally related to the co-pigmentation effect [41].

In addition to the hyperchromic effect, bathochromic shifts were recorded, representing a shift of the maximum absorbance wavelength ( $\lambda_{max}$ ) to longer wavelengths [49]. These shifts ranged from 2 to 9.5 nm, with the largest shift observed at the highest molar ratio of 1:500. Indicators of co-pigmentation included alterations in absorbance at  $\lambda_{max}$  (hyperchromic effect, M) and shifts in the maximum wavelength ( $\Delta\lambda_{max}$ , bathochromic shift). As co-pigments often demonstrated negligible absorbance in the visible spectrum, any detected alterations in the sample's absorbance or peak wavelength could be ascribed to the co-pigmentation effect [28]. Co-pigmentation induced hyperchromic and bathochromic effects, consistent with previous studies, the co-pigmentation of black rice anthocyanins with flavonoids [24]. Bathochromic shifts and hyperchromic effects were observed in blueberry wines with several co-pigments, including caffeic acid, syringic acid, and quercetin, with caffeic acid demonstrating the most significant impact [28].

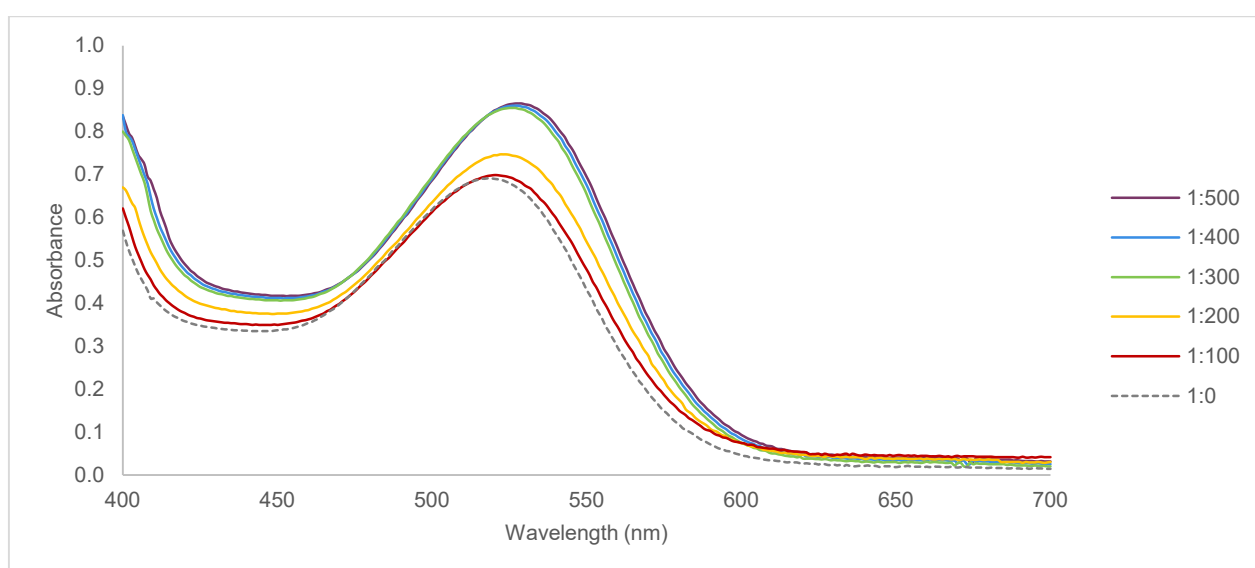


**Figure 3** The spectrum of RPAE in various molar ratios of GA as co-pigment in pH 1.

The interaction between RPAE and GA generated both effects, with the most pronounced results noted at the highest pigment-to-co-pigment ratio. Although such high ratios were not commonly achievable in natural plant systems, the co-pigmentation phenomenon visibly enhanced the color intensity, even detectable by the naked eye. This increase in color intensity strongly correlated with the hyperchromic effect, as presented in

**Table 3** and in the earlier discussion of  $L^*$ ,  $a^*$ ,  $b^*$  and  $\Delta E^*$ . This correlation is attributed to the molecular interactions between the chromophore groups of RPAE and GA, which promoted the expected color enhancement [28]. The results align with previous studies, including the co-pigmentation of black chokeberry anthocyanins with polyphenols, improving color intensity and stability [41].

**Table 3** Maximum wavelength, hyperchromic effect, bathochromic shift, and color intensity of RPAE without and with GA co-pigmentation.

Molar ratio	$\lambda_{\max}$ , nm	Hyperchromic effect ( $\Delta A$ ), %	Bathochromic shift ( $\Delta \lambda_{\max}$ )	Color Intensity
1:0	$518.5 \pm 0.5^a$	-	-	$1.07 \pm 0.10^a$
1:100	$520.5 \pm 0.5^b$	$1.16 \pm 0.12^a$	$2 \pm 0.5^a$	$1.13 \pm 0.09^{ab}$
1:200	$523 \pm 0.5^c$	$7.97 \pm 0.26^b$	$4.5 \pm 0.5^b$	$1.21 \pm 0.09^b$
1:300	$526 \pm 0.5^d$	$22.46 \pm 0.38^c$	$7.5 \pm 0.5^c$	$1.35 \pm 0.09^c$
1:400	$527 \pm 0.5^e$	$22.61 \pm 0.25^c$	$8.5 \pm 0.5^d$	$1.37 \pm 0.09^c$
1:500	$528 \pm 0.5^f$	$22.90 \pm 0.51^c$	$9.5 \pm 0.5^e$	$1.39 \pm 0.07^c$

Values with differing superscripts within the same column indicate statistically significant differences (DMRT,  $p \leq 0.05$ ).

#### FTIR of RPAE with GA as co-pigment

The FTIR spectrum of RPAE co-pigmented with GA was presented in **Figure 4**. A band associated with the carbonyl group was observed in the wavenumber range of 1,600 to 1,700  $\text{cm}^{-1}$ . In **Figure 4**, a shift in the band from 1,634 to 1,651  $\text{cm}^{-1}$  was noted, which indicated an interaction between the carbonyl groups of anthocyanins with GA. This interaction could alter the conjugation and electron resonance within the anthocyanins molecules, thereby influencing the pigment's stability and color properties. Co-pigmentation involved non-covalent interactions between anthocyanins and co-pigment molecules, leading to modifications to the pigment's optical characteristics through hydrogen bonding, Van der Waals interactions, and  $\pi$ - $\pi$  stacking between aromatic

rings [28]. The formation of stable pigment-cofactor interactions relied on the chemical structure of proton donors, proton acceptors, and their aromatic rings. An efficient co-pigment necessitated a suitably extensive  $\pi$ -conjugated system to augment interactions through hydrogen bond donor/acceptor groups, such as -OH and C=O groups, as well as  $\pi$ - $\pi$  stacking interactions [28]. Furthermore, the band in the O-H and N-H stretching region (3,200 - 3,600  $\text{cm}^{-1}$ ) indicated the presence of hydroxyl groups in hydrogen bonding. This similarity across samples was reflected at the wavenumber 3,445  $\text{cm}^{-1}$ . The prominent absorption band observed in the 3,200 to 3,600  $\text{cm}^{-1}$  range was ascribed to the stretching vibrations of -OH groups, particularly the phenolic hydroxyl groups present in anthocyanins [50].

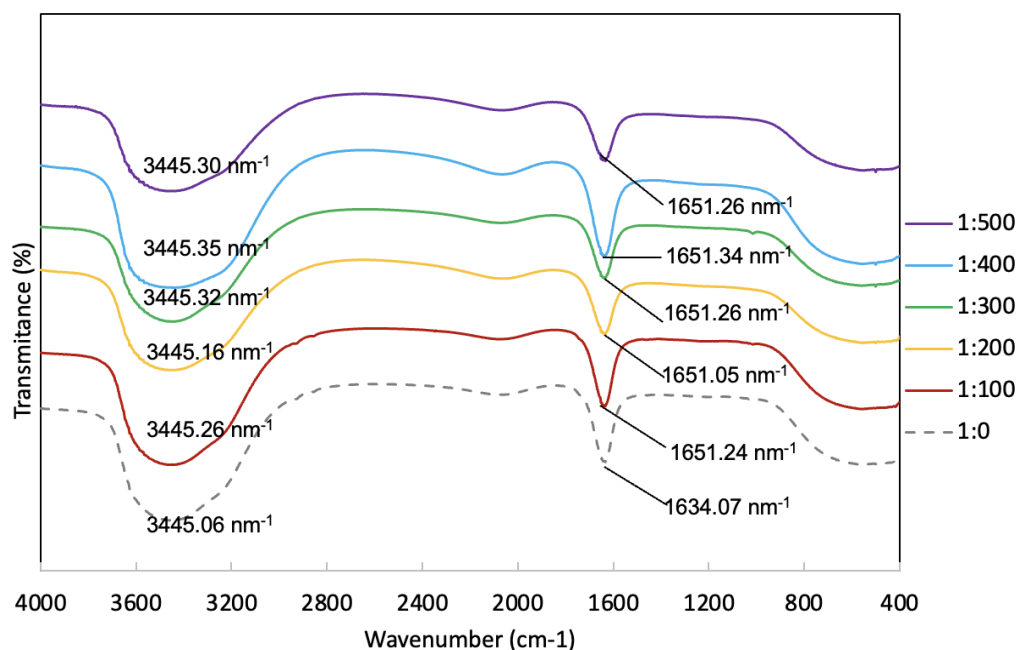


**Figure 4** FTIR of RPAE with GA as co-pigment.

Co-pigment chemical groups with 1 or more phenolic rings, including flavonols (e.g., quercetin), phenolic acids (e.g., caffeic acid, ferulic acid, GA, and protocatechuic acid), and hydroxybenzoic acids (e.g., syringic acid and vanillic acid), were used to improve the stability of anthocyanins [28,41,51]. These compounds were characterized by hydroxyl and/or carbonyl oxygen groups, facilitating their interaction with anthocyanins through hydrogen bonding or charge transfer interactions, thereby promoting co-pigmentation [28]. Intramolecular interactions primarily arose from the self-association of anthocyanins. These interactions comprised the establishment of hydrogen bonds, hydrophobic forces, Van der Waals forces, and ionic interactions between anthocyanins and non-anthocyanins co-pigments, such as phenolic acids, proteins, metal ions, and polysaccharides [49]. The anthocyanins-co-pigment relationship was driven by weak molecular forces, including hydrogen bonding and hydrophobic effects, particularly  $\pi$ - $\pi$  interactions between the polarized orbitals of aromatic rings. Hydrogen bonding and Van der Waals interactions, particularly vertical stacking, between the planar, polarizable anthocyanins cores served as the primary forces in co-pigmentation. Anthocyanins molecules were protected from water's nucleophilic attack through non-covalent interactions [49,52]. Co-pigmentation has

the potential to enhance the  $\pi$ -conjugated system, thereby facilitating  $\pi$ - $\pi$  stacking interactions and the presence of hydrogen bond donor/acceptor groups, such as -OH and C=O [53]. Co-pigmentation enhanced anthocyanins stability by facilitating  $\pi$ - $\pi$  interactions between electron-rich co-pigments and the flavylum cation of anthocyanins [23,24]. RPAE co-pigmentation with GA improved the stability of anthocyanins through carbonyl interactions while maintaining their pH-dependent color-changing properties. This indicated the potential of GA-copigmented RPAE as a pH-sensitive dye for applications in intelligent packaging systems.

## Conclusions

In conclusion, this study evaluated the RPAE and investigated its co-pigmentation with GA to enhance color stability and pH sensitivity. The findings showed that RPAE purified with Sephadex LH-20 increased TAC by up to 22.28 %, with a 157.50 mg CyE/100 g extract content. Further improvements in purity can be achieved by incorporating additional purification stages. The identified anthocyanins were cyanidin, delphinidin, and pelargonidin derivatives. Co-pigmentation with GA reduced the degradation of TAC over time. Moreover, RPAE with GA as a co-pigment demonstrated higher color intensity and greater pH sensitivity, with more distinct color differences across pH levels than RPAE

without co-pigmentation. This was demonstrated by an increase in the  $a^*$  value at low pH and a decrease in the  $b^*$  and  $L^*$  values at high pH. Additionally, co-pigmentation produced hyperchromic and bathochromic effects, probably due to hydrogen bonds through the carbonyl group of anthocyanins. These findings suggest that GA co-pigmentation significantly enhances the visual and chemical stability of RPAE, demonstrating strong potential as a pH-sensitive dye for intelligent food packaging applications. Furthermore, this study provides a foundation for future research on color changes in RPAE applied to food products undergoing degradation or the degradation patterns of alkaline compounds, such as ammonia and total basic nitrogen. Ultimately, these insights are expected to contribute to advancing intelligent food packaging solutions.

#### Acknowledgments

The authors gladly recognized the financial support provided by the Ministry of Education, Culture, Research, and Technology of the Republic of Indonesia for the Doctoral Dissertation Research grant in 2024 under contract numbers 048/E5/PG.02.00.PL/2024 and 2783/UN1/DITLIT/PT.01.03/2024.

#### References

- [1] H Yong and J Liu. Recent advances in the preparation, physical and functional properties, and applications of anthocyanins-based active and intelligent packaging films. *Food Packaging and Shelf Life* 2020; **26**, 100550.
- [2] D Zheng, S Cao, D Li, Y Wu, P Duan, S Liu, X Li, X Zhang and Y Chen. Fabrication and characterization of chitosan/anthocyanin intelligent packaging film fortified by cellulose nanocrystal for shrimp preservation and visual freshness monitoring. *International Journal of Biological Macromolecules* 2024; **264(2)**, 130692.
- [3] S Roy and J W Rhim. Anthocyanin food colorant and its application in pH-responsive color change indicator films. *Colloids and Surfaces B: Biointerfaces* 2021; **61(14)**, 2297-2325.
- [4] Q Ma, X Lu, W Wang, MA Hubbe, Y Liu, J Mu, J Wang, J Sun and O Rojas. Recent developments in colorimetric and optical indicators stimulated by volatile base nitrogen to monitor seafood freshness. *Food Packaging and Shelf Life* 2021; **28(59)**, 100634.
- [5] Y Bao, H Cui, J Tian, Y Ding, Q Tian, W Zhang, M Wang, Z Zang, X Sun, D Li, X Si and B Li. Novel pH sensitivity and colorimetry-enhanced anthocyanin indicator films by chondroitin sulfate co-pigmentation for shrimp freshness monitoring. *Food Control* 2022; **131(4)**, 108441.
- [6] I Choi, H Choi, J S Lee and J Han. Novel color stability and colorimetry-enhanced intelligent CO<sub>2</sub> indicators by metal complexation of anthocyanins for monitoring chicken freshness. *Food Chemistry* 2023; **404(A)**, 134534.
- [7] E Mohammadian, M Alizadeh-Sani and SM Jafari. Smart monitoring of gas/temperature changes within food packaging based on natural colorants. *Comprehensive Reviews in Food Science and Food Safety* 2020; **19(6)**, 2885-2931.
- [8] D Wu, M Zhang, H Chen and B Bhandari. Freshness monitoring technology of fish products in intelligent packaging. *Critical Reviews in Food Science and Nutrition* 2021; **61(8)**, 1279-1292.
- [9] A Duan, J Yang, L Wu, T Wang, Q Liu and Y Liu. Preparation, physicochemical and application evaluation of raspberry anthocyanin and curcumin based on chitosan/starch/gelatin film. *International Journal of Biological Macromolecules* 2022; **220(19)**, 147-158.
- [10] X Zhou, X Yu, F Xie, Y Fan, X Xu, J Qi, G Xiong, X Gao and F Zhang. pH-responsive double-layer indicator films based on konjac glucomannan/camellia oil and carrageenan/anthocyanin/curcumin for monitoring meat freshness. *Food Hydrocolloid* 2021; **118(3)**, 106695.
- [11] L Gao, P Liu, L Liu, S Li, Y Zhao, J Xie and H Xu.  $\kappa$ -carrageenan-based pH-sensing films incorporated with anthocyanins or/and betacyanins extracted from purple sweet potatoes and peels of dragon fruits. *Process Biochemistry* 2022; **121**, 463-480.
- [12] A Etxabide, P A Kilmartin and J I Maté. Color stability and pH-indicator ability of curcumin, anthocyanin and betanin containing colorants under different storage conditions for intelligent

- packaging development. *Food Control* 2021; **121**, 107645.
- [13] Q Tang, J Hu, S Li, S Lin, Y Tu, X Gui and Y Dong. Preparation of an aramid nanofiber-reinforced colorimetric hydrogel employing natural anthocyanin as an indicator for shrimp and fish spoilage monitoring. *European Polymer Journal* 2023; **187(21)**, 111889.
- [14] The Central Statistics Agency of Indonesia (BPS), Fruit Crop Production, Available at <https://www.bps.go.id/id/statistics-table/2/NjIjMg==/produksi-tanaman-buah-buahan.html>, accessed September 2024.
- [15] A Nurkhasanah, T Fardad, C Carrera, W Setyaningsih and M Palma. Ultrasound-assisted anthocyanins extraction from pigmented corn: Optimization using response surface methodology. *Methods and Protocols* 2023; **6(4)**, 69,
- [16] J Sun, H Peng, W Su, J Yao, X Long and J Wang. Anthocyanins extracted from rambutan (*nephelium lappaceum* L.) pericarp tissues as potential natural antioxidants. *Journal of Food Biochemistry* 2011; **35(5)**, 1461-1467.
- [17] BR Albuquerque, J Pinela, MI Dias, C Pereira, J Petrovic, M Sokovic, RC Calhelha, MBP Oliveira, ICFR Ferreira and L Barros. Valorization of rambutan (*Nephelium lappaceum* L.) peel: Chemical composition, biological activity, and optimized recovery of anthocyanins. *Food Research International* 2023; **165**, 112574.
- [18] J Liao, B Peng, X Chu and G Yu. Effects of process parameters on the extraction of total anthocyanins from purple sweet potatoes by ultrasound with wide frequency and its kinetics study. *Journal of Food Processing and Preservation* 2022; **46(7)**, e16732.
- [19] C Hernández, J Ascacio-Valdés, HDL Garza, J Wong-Paz, CN Aguilar, GC Martínez-Ávila, C Castro-López and A Aguilera-Carbó. Polyphenolic content, *in vitro* antioxidant activity and chemical composition of extract from *Nephelium lappaceum* L. (Mexican rambutan) husk. *Asian Pacific Journal of Tropical Medicine* 2017; **10(12)**, 1201-1205.
- [20] H He, L Wang, H Huang and Y Li. A novel gallic acid-based anthocyanin *Electrospun* sensor for monitoring shrimp freshness. *Food Analytical Methods* 2024; **17(5)**, 689-700.
- [21] Y Osawa. *Copigmentation of anthocyanins*. In: P. Markakis (Ed.). *Anthocyanins as food colors*. Academic Press, New York, 1982, p. 41-86.
- [22] R Becerril, C Nerín and F Silva. Bring some colour to your package: Freshness indicators based on anthocyanin extracts. *Trends in Food Science & Technology* 2021; **111(11)**, 495-505.
- [23] X Lv, L Li, X Lu, W Wang, J Sun, Y Liu, J Mu, Q Ma and J Wang. Effects of organic acids on color intensification, thermodynamics, and copigmentation interactions with anthocyanins. *Food Chemistry* 2022; **396(3)**, 133691.
- [24] S Raharjo, FA Purwandari, P Hastuti and K Olsen. Stabilization of black rice (*Oryza Sativa*, L. Indica) anthocyanins using plant extracts for Copigmentation and maltodextrin for encapsulation. *Journal Food Science* 2019; **84(7)**, 1712-1720.
- [25] MT Escribano-Bailón and C Santos-Buelga. Anthocyanin copigmentation-evaluation, mechanisms and implications for the colour of red wines. *Current Organic Chemistry* 2012; **16(6)**, 715-723.
- [26] F Sari. The copigmentation effect of different phenolic acids on *berberis crataegina* anthocyanins. *Journal of Food Processing and Preservation* 2016; **40(3)**, 422-430.
- [27] RJ Robbins. Phenolic acids in foods: An overview of analytical methodology. *Journal of Agricultural and Food Chemistry* 2003; **51(10)**, 2866-2887.
- [28] X Sun, S Shokri, B Gao, Z Xu, B Li, T Zhu, Y Wang and J Zhu. Improving effects of three selected co-pigments on fermentation, color stability, and anthocyanins content of blueberry wine. *LWT* 2022; **156(4)**, 113070.
- [29] HH Nurhuda, MY Maskat, S Mamot, J Afiq and A Aminah. Effect of blanching on enzyme and antioxidant activities of rambutan (*nephelium lappaceum*) peel. *International Food Research Journal* 2013; **20(4)**, 1725-1730.
- [30] M Ziabakhsh Deylami, R Abdul Rahman, CP Tan, J Bakar and L Olusegun. Effect of blanching on enzyme activity, color changes, anthocyanin

- stability and extractability of mangosteen pericarp: A kinetic study. *Journal of Food Engineering* 2016; **178**, 12-19.
- [31] AOAC International and GWL Jr. *Official methods of analysis of the association of official analytical chemists*. Oxford University Press, Washington DC, 1999.
- [32] MM Giusti and RE Wrolstad. Characterization and measurement of anthocyanins by UV-visible spectroscopy. *Current Protocols in Food Analytical Chemistry* 2001. <https://doi.org/10.1002/0471142913.faf0102s00>
- [33] Husniati, J Permana and T Suhartati. Antioxidant enrichment for artificial red rice by natural red pigment extract from *Rhoeo discolor* L. her. *Biopropal Industri* 2020; **11(1)**, 33-40.
- [34] H Xue, J Tan, Q Li, J Tang and X Cai. Ultrasound-assisted enzymatic extraction of anthocyanins from raspberry wine residues: Process optimization, isolation, purification, and bioactivity determination. *Food Analytical Methods* 2021; **14(7)**, 1369-1386.
- [35] YP Nusantara, LN Lestario and Y Martono. Effect addition of gallic acid as copigment for black mulberry anthocyanin (*Morus nigra* L.) towards thermal stability. *Agritech* 2017; **37(4)**, 428-436.
- [36] S Klongdee and U Klinkesorn. Optimization of accelerated aqueous ethanol extraction to obtain a polyphenol-rich crude extract from rambutan (*Nephelium lappaceum* L.) peel as natural antioxidant. *Scientific Reports* 2022; **12(1)**, 21153.
- [37] TC Wallace and MM Giusti. Anthocyanins-nature's bold, beautiful, and health-promoting colors. *Foods* 2019; **8(11)**, 550.
- [38] LD Vedova, G Ferrario, F Gado, A Altomare, M Carini, P Morazzoni, G Aldini and G Baron. Liquid chromatography-high-resolution mass spectrometry (LC-HRMS) profiling of commercial enocianina and evaluation of their antioxidant and anti-inflammatory activity. *Antioxidants* 2022; **11(6)**, 1187.
- [39] A Ningrum, AW Perdani, S Supriyadi, HSH Munawaroh, S Aisyah and E Susanto. Characterization of tuna skin gelatin edible films with various plasticizers-essential oils and their effect on beef appearance. *Journal of Food Processing and Preservation* 2021; **45(9)**, e15701.
- [40] S Naghdi, M Rezaei and M Abdollahi. A starch-based pH-sensing and ammonia detector film containing betacyanin of paperflower for application in intelligent packaging of fish. *International Journal of Biological Macromolecule* 2021; **191**, 161-170.
- [41] D Klisurova, I Petrova, M Ognyanov, Y Georgiev, M Kratchanova and P Denev. Co-pigmentation of black chokeberry (*Aronia melanocarpa*) anthocyanins with phenolic co-pigments and herbal extracts. *Food Chemistry* 2019; **279**, 162-170.
- [42] H Xue, L Shen, X Wang, C Liu, C Liu, H Liu and X Zheng. Isolation and purification of anthocyanin from blueberry using macroporous resin combined sephadex LH-20 techniques. *Food Science and Technol Research* 2019; **25(1)**, 29-38.
- [43] S Torgbo, U Sukatta, P Kamonpatana and P Sukyai. Ohmic heating extraction and characterization of rambutan (*Nephelium lappaceum* L.) peel extract with enhanced antioxidant and antifungal activity as a bioactive and functional ingredient in white bread preparation. *Food Chemistry* 2022; **382**, 132332.
- [44] C Hernández-Hernández, CN Aguilar, R Rodríguez-Herrera, AC Flores-Gallegos, J Morlett-Chávez, M Govea-Salas and JA Ascacio-Valdés. Rambutan (*Nephelium lappaceum* L.): Nutritional and functional properties. *Trends in Food Science & Technology* 2019; **85**, 201-210.
- [45] Y Jiang, J Pei, Y Zheng, YJ Miao, BZ Duan and LF Huang. Gallic acid: A potential anti-cancer agent. *Chinese Journal of Integrative Medicine* 2022; **28(7)**, 661-671.
- [46] B J Qian, J H Liu, S J Zhao, J X Cai and P Jing. The effects of gallic/ferulic/caffeic acids on colour intensification and anthocyanin stability. *Food Chemistry* 2017; **228**, 526-532.
- [47] SS Rosales-Murillo, J Sánchez-Bodón, SLH Olmos, MF Ibarra-Vázquez, LG Guerrero-Ramírez, L Pérez-Álvarez and JL Vilas-Vilela. Anthocyanin-loaded polymers as promising nature-based, responsive, and bioactive materials. *Polymers* 2024; **16(1)**, 163.

- [48] F Zeng, Y Ye, J Liu and P Fei. Intelligent pH indicator composite film based on pectin/chitosan incorporated with black rice anthocyanins for meat freshness monitoring. *Food Chemistry X* 2022; **17**, 100531.
- [49] E Gençdag, EE Özdemir, K Demirci, A Görgüç and FM Yılmaz. Copigmentation and stabilization of anthocyanins using organic molecules and encapsulation techniques. *Current Plant Biology* 2022; **29**, 100238.
- [50] X Chen, Q Gao, S Liao, Y Zou, J Yan and Q Li. Co-pigmentation mechanism and thermal reaction kinetics of mulberry anthocyanins with different phenolic acids. *Foods* 2022; **11(23)**, 3806.
- [51] L Zhang, W Wang, X Yue, GS Wu, P Yue and X Gao. Gallic acid as a copigment enhance anthocyanin stabilities and color characteristics in blueberry juice. *Journal of Food Science and Technology* 2020; **57(4)**, 1405-1414.
- [52] H Zou, Y Ma, Z Xu, X Liao, A Chen and S Yang. Isolation of strawberry anthocyanins using high-speed counter-current chromatography and the copigmentation with catechin or epicatechin by high pressure processing. *Food Chemistry* 2018; **247**, 81-88.
- [53] P Trouillas, J C Sancho-García, V De Freitas, J Gierschner, M Otyepka and O Dangles. Stabilizing and modulating color by copigmentation: Insights from theory and experiment. *Chemical Reviews* 2016; **116(9)**, 4937-4982.